Nuclear Engineering and Technology 56 (2024) 241–246

Contents lists available at ScienceDirect

Nuclear Engineering and Technology

journal homepage: www.elsevier.com/locate/net

Original Article

Calculation of X-ray attenuation coefficients for normal and cancerous breast tissues

Aysun Böke

Balıkesir University, Faculty of Arts and Sciences, Department of Physics, Çağış Campus, Balıkesir, Turkey

ARTICLE INFO

Keywords:
X-ray scatter
Photon attenuation
Tissue
Breast cancer

ABSTRACT

The study was carried out by numerical integration based on the diffraction properties and elemental composition. The elemental compositions of breast tissues in the literature were tested. The photon attenuation coefficients calculated using the recent elemental composition were found within 0.2−16% for adipose tissue and within 0.04−17% for glandular tissue with the experimental reference data. The attenuation coefficients of cancerous breast tissue calculated according to the elemental content previously measured in breast cancer patients were found within 0−17% with experimental data in the literature. The attenuation coefficients are of great interest to medical research. To calculate realistic attenuation coefficients, the characteristic coherent scatter, which is most intense at small angles, must be considered. For this reason, experimentally measured form factor data were reviewed, and the most compatible one with the theoretical form factor data produced in this study was used at low momentum transfer x ($0 < x \leq 8$ nm^{-1}). The differential linear coherent scattering distributions were calculated for an energy value of 17.44 keV and compared with their experimental counterparts.

1. Introduction

The attenuation coefficients are commonly employed in Monte Carlo modeling and simulation and have recently been reported by some researchers [1–17]. The photon attenuation coefficient information is very important for inter-tissue image quality. According to the World Health Organization, mammography has proven to be an effective method of screening for breast cancer. It is associated with the difference between the attenuation coefficients of breast tissues. By revealing the scattering characteristics of each tissue in the breast, it is possible to determine the small differences in the attenuation properties that give values close to each other and to end the mistakes in mammography. Thus, it is ensured that the dose given to the patient is adjusted more accurately.

The attenuation coefficients of breast tissues were calculated by Hammerstein et al. [18] and Woodard & White [19]. White et al. [20] experimentally obtained the attenuation coefficients for energy values between 9.88 and 59.32 keV. Johns & Yaffe [21] made measurements to determine the attenuation properties of normal and neoplastic breast tissues at energy values between 18 and 110 keV. At energies lower than 40 keV, fibroglandular tissue was found to be significantly different from cancerous tissue. Carroll et al. [22] made measurements for energy values between 14 and 18 keV to determine the attenuation properties of normal and cancerous breast tissues. Al-Bahri & Spyrou [23] presented experimental data at 59.5 keV energy. Chen et al. [24] stated that the measurement results of adipose and fibrous tissues in the 15−26.5 keV energy range are the same as the data in the literature, and there is no significant difference between fibrous and tumor tissues. Tomal et al. [25] tried to experimentally determine the attenuation properties of normal and neoplastic breast tissues at energy values between 8 and 30 keV and found that the attenuation coefficients of neoplastic breast tissues were slightly higher than those of glandular tissues. The important explanation by Tomal [26] for the fact that the glandular attenuation graph is different from that of tumor tissues is that tumor formations have higher atomic number elements and densities than glandular ones. Mirji et al. [27] made measurements to determine the attenuation coefficients of healthy and cancerous breast tissues of patients in different age groups at energy values between 8 and 18 keV and showed that the attenuation coefficient values of cancerous breast tissue are higher than those of healthy breast tissues. Fredenberg et al. [28] made measurements to determine the photon attenuation properties of solid breast lesions at energy values between 15 and 40 keV. Fredenberg et al. [29] measured the x-ray attenuation coefficients at energy values between 15 and 40 keV. Soares et al. [30] presented the photon attenuation coefficients graphically.

It is known that the elemental contents of tissues differ considerably among different people [31,32]. Biological age, sex, metabolism, dietary

E-mail address: aysun@balikesir.edu.tr.

https://doi.org/10.1016/j.net.2023.09.031
Received 3 May 2023; Received in revised form 26 August 2023; Accepted 24 September 2023
Available online 22 October 2023

habits, and health status play an important role in determining the elemental tissue content. The elemental knowledge of body tissues cannot be thought to be fixed, and variation must be considered [32]. In particular, where the identification of tissue occurs by coherent scattering, this variation should always be taken into consideration [32].

The most comprehensive work on elemental knowledge of breast tissues was published by Hammerstein et al. [18]. In addition to this, Woodard and White [19] made a few measurements for glandular tissue. These data were declared in the ICRU [33] report. Poletti et al. [34] experimentally revealed the elemental contents to determine the angular scattering distributions of adipose and glandular tissues. Poletti et al. [35] obtained the elemental composition of cancerous breast tissues by elemental analysis.

In this study, the elemental compositions of breast tissues in the literature were tested. The theoretical results of healthy breast tissues carried out by using the recent elemental composition [32] and the diffraction patterns [34] were found to be more compatible with the experimental data. The coherent scatter distributions and attenuation coefficients of cancerous breast tissue were determined from experimentally measured elemental composition [35] and diffraction patterns [34]. Theoretical differential linear coherent scatter distributions of normal and cancerous breast tissues were calculated and compared with their experimental counterparts in Figs. 1–3 for an energy value of 17.44 keV. Theoretical total linear attenuation coefficients were calculated for 1–50 keV energy values. The results were listed in Table 1 and compared in Tables 2–4 with the literature. In general, good agreement is obtained. This type of study is new. To the best of our knowledge, it is the first time that such a theoretical study has been obtained by including diffraction effects and using the recent elemental contents of breast tissues. Therefore, this work will provide valuable knowledge.

Table 1
The theoretical linear attenuation coefficients (μ) of the adipose, glandular, and cancerous breast tissues, respectively.

E (keV)	μ (cm^{-1}) $_{Adipose}$	μ (cm^{-1}) $_{Glandular}$	μ (cm^{-1}) $_{Cancerous}$
1	2359,8522	3654,0526	3696,3690
2	338,4207	546,3685	548,9437
3	103,4337	169,9149	170,3502
4	43,8844	72,5599	72,7506
5	22,4776	37,2478	37,3577
6	13,0109	21,4940	21,5789
7	9,2506	15,2441	15,3226
8	5,4971	8,9908	9,0597
9	4,2056	6,8054	6,8704
10	2,8853	4,4102	4,6628
11	2,4878	3,9665	4,0208
12	2,1115	3,3351	3,3853
13	1,7317	2,7054	2,7521
14	1,3522	2,0703	2,1143
15	0,9717	1,4395	1,4816
16	0,8806	1,2962	1,3285
17	0,7922	1,1469	1,1802
18	0,7036	0,9939	1,0316
19	0,6125	0,8458	0,8825
20	0,5228	0,6964	0,7321
21	0,4953	0,6590	0,6937
22	0,4707	0,6207	0,6547
23	0,4481	0,5832	0,6165
24	0,4250	0,5465	0,5792
25	0,4026	0,5097	0,5419
26	0,3787	0,4730	0,5047
27	0,3558	0,4358	0,4671
28	0,3329	0,3985	0,4294
29	0,3098	0,3620	0,3925
30	0,2870	0,3260	0,3561
31	0,2804	0,3164	0,3461
32	0,2744	0,3070	0,3364
33	0,2685	0,2981	0,3272
34	0,2624	0,2892	0,3179
35	0,2566	0,2803	0,3086
36	0,2505	0,2714	0,2994
40	0,2266	0,2362	0,2623
45	0,2128	0,2199	0,2438
50	0,2011	0,2044	0,2263

2. Methods

2.1. The attenuation coefficient

The attenuation coefficients include the following processes: coherent (Rayleigh) scattering, incoherent (Compton) scattering, and photoelectric absorption, with the participation of each photon interaction in the interaction with the matter of low-energy x-rays. The linear attenuation coefficient μ (cm^{-1}) is proportional to the photon interaction cross-section per molecule. This relationship is reported by Hubbell [36] as follows,

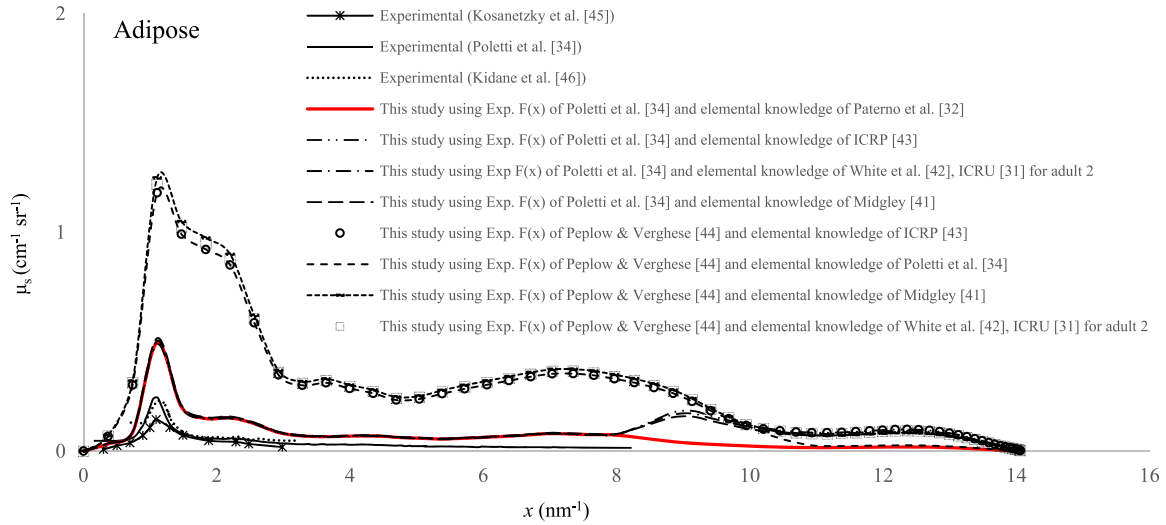

Fig. 1. Theoretical linear differential coherent scattering coefficients (μ_s) compared with experimental data in the literature for adipose breast tissue.

Table 2
The linear attenuation coefficients of adipose breast tissue μ (cm^{-1}) calculated in this study are compared with the references.

E (keV)	This study	References
8	5,4971	5,70 (5,28–6,70) [25]
9,88	3,0437	2,907 [20]
11	2,4878	2,28 (2,04–2,92) [25]
15	0,9717	0,902–0,906 [29]
		0,978 (0,903–1,169) [25]
17,44	0,7532	0,72 [32]
		0,64 [34]
20	0,5228	0,494 (0,455–0,559) [25]
		0,484–0,486 [29]
25	0,4026	0,338–0,339 [29]
27	0,3558	0,317 [47]
30	0,2870	0,280 (0,260–0,304) [25]
		0,273–0,274 [29]
35	0,2566	0,239–0,240 [29]
39,91	0,2271	0,2156 [20]
40	0,2266	0,219–0,220 [29]
		0,212–0,218 [21]
59,5	0,1755	0,169–0,259 [23]

$$\mu\left(cm^{-1}\right)=\sigma\left[\frac{barn}{molecule}\right].\frac{N_A\rho}{M}.10^{-24} \quad (1)$$

Here, N_A is Avogadro's constant, ρ is the density, M is the molecular weight, and σ is the photon interaction cross-section. The coherent (Rayleigh) scattering, incoherent (Compton) scattering, and photoelectric absorption cross-sections per molecule were calculated by Ref. [37].

The differential linear coherent scattering coefficient μ_s (x) of a molecule per unit solid angle is expressed by the following equation,

$$\mu_s(x)=\frac{N_A\rho}{M}\left[\frac{d\sigma^T(\theta)}{d\Omega}F_m^2(x)\right] \quad (2)$$

where $F_m(x)$ is the molecular form factor of most complex substances, $d\sigma_T$ is the differential Thomson scattering cross-section per free electron, and $d\Omega$ is the differential solid angle.

For small values of the momentum transfer variable x, the Independent Atomic Model (IAM) [38] cannot be applied due to high interference effects. Therefore, the $F_m(x)$ values for $\sim x \leq 8$ nm^{-1} should be taken from experimental data to include interference effects. Experimental data are not available for values greater than $x > 8$ nm^{-1}. For large x values, the IAM can be applied because of the agreement between the experimental data and those obtained using the IAM. Thus, all the $F_m(x)$ values are created for all possible values of x. Experimental $F_m(x)$ data ($\sim x \leq 8$ nm^{-1}) and theoretical $F_m(x)$ data ($\sim x > 8$ nm^{-1}) should be compatible and provide integrity. The MRFF data [39] is used to ensure this integrity. The theoretical form factor obtained with the MRFF theory agrees better with the experimental form factor than those obtained with Hubbell et al. [40]'s relativistic and Hubbell & Øverbø [38]'s nonrelativistic form factor theories.

3. Results

The elemental compositions of different researchers [19, 31–35, 41–43] were tested. The molecular form factor values of adipose and glandular tissues were obtained theoretically for each of the elemental contents. The molecular form factor of cancerous breast tissue was calculated using the experimental elemental composition by Poletti et al. [35].

The theoretical form factors obtained with the IAM ensure an approximation in the interval $\sim x = 8$ to 1000 nm^{-1}, where experimental data are not available. To take into account the characteristic x-ray diffraction effects, the experimental form factor data [34,44] were used in the interval $x = 0$ to 8 nm^{-1}. In the creation of the form factor data of cancerous tissue, experimental values of glandular tissue, which resemble carcinoma, were used for low x values as suggested by Poletti et al. [35].

The total linear attenuation coefficient as the sum of coherent, incoherent, and photoelectric effects was calculated by applying Eq. (1). The theoretical attenuation coefficients were listed in Table 1 and compared in Tables 2–4 with experimental data [20, 21, 23−25, 27−29, 34] and theoretical data [32].

The differential coherent scattering coefficient ($\mu_s(x)$) of a molecule per unit solid angle was calculated by applying Eq. (2). To test the accuracy of this theoretical study of breast tissues, the theoretical differential linear coherent scattering distribution μ_s ($cm^{-1}sr^{-1}$) as a function of x (nm^{-1}) was compared with its experimental counterpart [34,45,46]. The results were graphically shown in Figs. 1−3 for an energy value of 17.44 keV.

4. Discussion

When our theoretical total attenuation coefficient values were compared with the experimental values, discrepancies were found between 0.2 and 16% for adipose tissue, 0.04 and 17% for glandular tissue, and 0 and 17% for cancerous breast tissue. The margin of error in the experimental form factor [34] used in this study was reported to be between 5% and 7%. It is necessary to consider uncertainties in the attenuation coefficients measured by different researchers. Also, these differences may be due to changes in the composition of the tissues. As pointed out by Paterno et al. [32], the composition of a particular tissue may vary from individual to individual, while the composition of a particular tissue in an individual may vary from one part of the body to another in the same individual. As a result, in general, there is good agreement when considering the variation in tissue compositions and the possible experimental errors.

The differential linear coherent scattering distributions of breast tissues per unit solid angle give a wide peak in the range of $x = 0.3$ nm^{-1} and $x = 3.5$ nm^{-1}. Intramolecular effects are very important in this region. For example, adipose tissue in Fig. 1 peaks around ~1.1 nm^{-1}, glandular tissue in Fig. 2 peaks around ~1.5 nm^{-1}, and cancerous tissue in Fig. 3 peaks around ~1.6 nm^{-1}. As pointed out by Kosanetzky et al. [45] and Kidane [46], the sharp peak in the lower momentum transfer value of adipose tissue compared to glandular and malignant tissues is thought to be because adipose tissue contains a large number of fat cells and also has interference effects. As stated by Kosanetzky et al. [45], these differences, which are related to the molecular structure of the tissues, can have important effects on breast imaging. As seen in Fig. 1, the theoretical $\mu_s(x)$ values with Paterno et al. [32] compositions are closest to the experimental $\mu_s(x)$ values. The theoretical $\mu_s(x)$ values with the ICRP, ICRU, and Midgley's [41] compositions are close to the experimental $\mu_s(x)$ values but deviate from the experimental data at

Table 3
The linear attenuation coefficients of glandular breast tissue μ (cm^{-1}) calculated in this study are compared with the references.

E (keV)	This study	References
8	8,9908	9,38 (8,94–9,76) [25]
11	3,9665	3,80 (3,64–3,96) [25]
15	1,4395	1,55 (1,48–1,62) [25]
		1,69–1,73 [29]
17,44	1,0796	1,08 [34]
		1,07 [32]
		1,14 [21]
20	0,6964	0,783 (0,752–0,815) [25]
		0,825–0,845 [29]
25	0,5097	0,523–0,532 [29]
30	0,3260	0,388–0,394 [29]
		0,380 (0,364–0,397) [25]
35	0,2803	0,319–0,327 [29]
40	0,2362	0,280–0,281 [29]
59,5	0,1861	0,184–0,277 [23]

Table 4
The linear attenuation coefficients of cancerous breast tissue μ (cm^{-1}) calculated in this study are compared with the references.

E (keV)	This study	References
8	9,0597	10,97 (9,90–11,91) [25]
		10,58 (10,36–10,58) [27]
11	4,0208	4,36 (4,04 - 4,76) [25]
12	3,3853	4,06 (4,02–4,11) [27]
14	2,1143	2,53 (2,46–2,55) [27]
15	1,4816	1,564–1,653 [24]
		1,74 (1,60–1,90) [25]
		1,76 [28]
		1,74–1,80 [29]
16	1,3285	1,54–1,65 [27]
17	1,1802	1,149–1,223 [24]
18	1,0316	1,061–1,137 [21]
		1,13 (1,08–1,20) [27]
19	0,8825	0,866–1,005 [24]
20	0,7321	0,851–0,877 [29]
		0,859 [28]
		0,856 (0,812–0,921) [25]
		0,826–0,884 [21]
23	0,6165	0,598–0,660 [24]
25	0,5419	0,538–0,551 [29]
		0,519–0,552 [21]
26	0,5047	0,476–0,492 [24]
		0,541 [28]
26,5	0,4859	0,457–0,507 [24]
30	0,3561	0,398–0,406 [29]
		0,400 [28]
		0,404 (0,368–0,430) [25]
		0,387–0,408 [21]
35	0,3086	0,326–0,332 [29]
		0,327 [28]
40	0,2623	0,285–0,289 [29]
		0,286 [28]
		0,276–0,291 [21]
50	0,2263	0,233–0,245 [21]
59,5	0,2120	0,212–0,295 [23]

values larger than $x = 8$ nm^{-1}. For the glandular tissue in Fig. 2, although it is possible to say that the theoretical $\mu_s(x)$ values with Paterno et al. [32] and Poletti et al. [34] compositions are close to the experimental data, the $\mu_s(x)$ values with Paterno et al. [32] compositions are closer to the experimental data. As seen in Figs. 1 and 2, the theoretical $\mu_s(x)$ values obtained using the experimental form factor values by Peplow & Verghese [44] are considerably larger than the experimental $\mu_s(x)$ values. For the cancerous tissue in Fig. 3, the theoretical $\mu_s(x)$ values are close to the experimental $\mu_s(x)$. As a result, these differences in the magnitude of the theoretical $\mu_s(x)$ values may vary depending on the choice of the elemental composition and experimental form factor.

The compatibility of our results with the experimental data proves the accuracy of our calculations. The most important step in these calculations shows us how important coherent scattering calculations are. The most important step of the coherent scattering calculation is to determine the breast tissue's most probable elemental content. Apart from the elemental content, another important part is the selection of experimental form factors used to incorporate diffraction effects into calculations. It is also important to use the MRFF theory to ensure the integrity of the experimental and theoretical form factor values. Thus, the best result was achieved by determining both the elemental content and the form factor.

In calculations of molecular cross-sections and attenuation coefficient values, we took into account intra-molecular effects. In the literature, total cross sections and attenuation coefficients are calculated by the XCOM database [47], which pertains to isolated neutral atoms and does not take molecular. With this, the XCOM database neglects the effects of coherent scatter diffraction. The lack of this effect plays a significant role in the coherent scattering and the total attenuation coefficient calculations. It is important to accurately calculate coherent scatter. Since the coherent differential scattering cross-sections and form factors change very drastically, logarithmic region selection has been made in the numerical integration in the small angle and low energy regions. By applying the logarithmic scale, the integration mesh points are increased. Thus, smaller angle values are also taken into account.

5. Conclusions

In this study, the complex molecular structures of healthy and cancerous breast tissues were investigated. It has been found that the elemental compositions of healthy human breast tissues published recently by Paterno et al. [32] are most compatible with the experimental results. The calculations for cancerous breast tissue were obtained based on the elemental content of cancerous breast tissue experimentally measured by Poletti et al. [35]. Another important part is the inclusion of diffraction effects in the calculations. The experimentally measured form factor data by Poletti et al. [34] were found to be the most compatible with the form factor data obtained theoretically

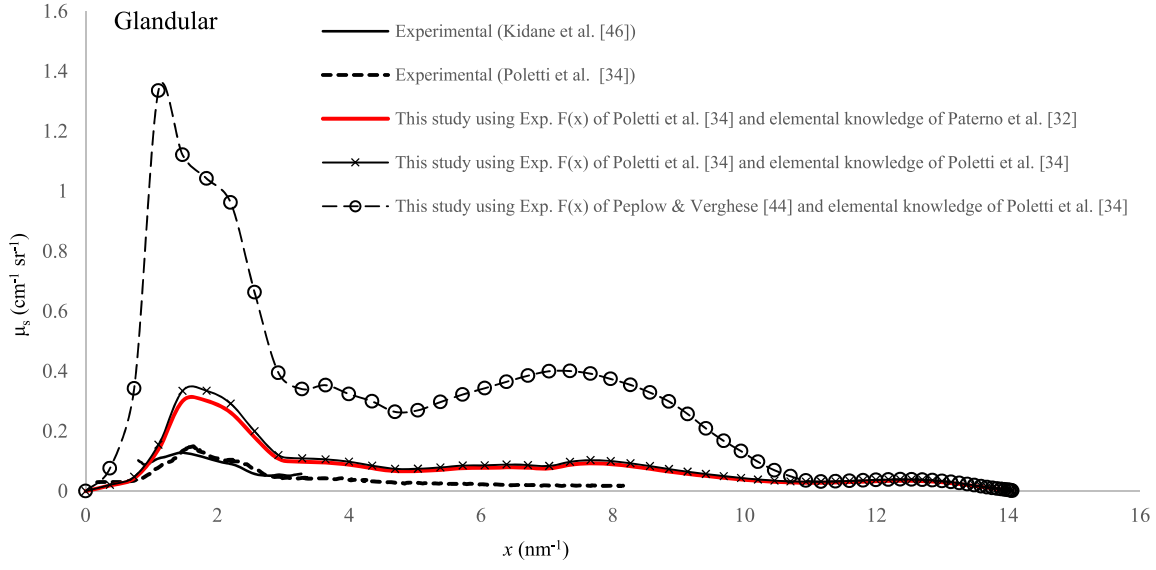

Fig. 2. Theoretical linear differential coherent scattering coefficients (μ_s) compared with experimental data in the literature for glandular breast tissue.

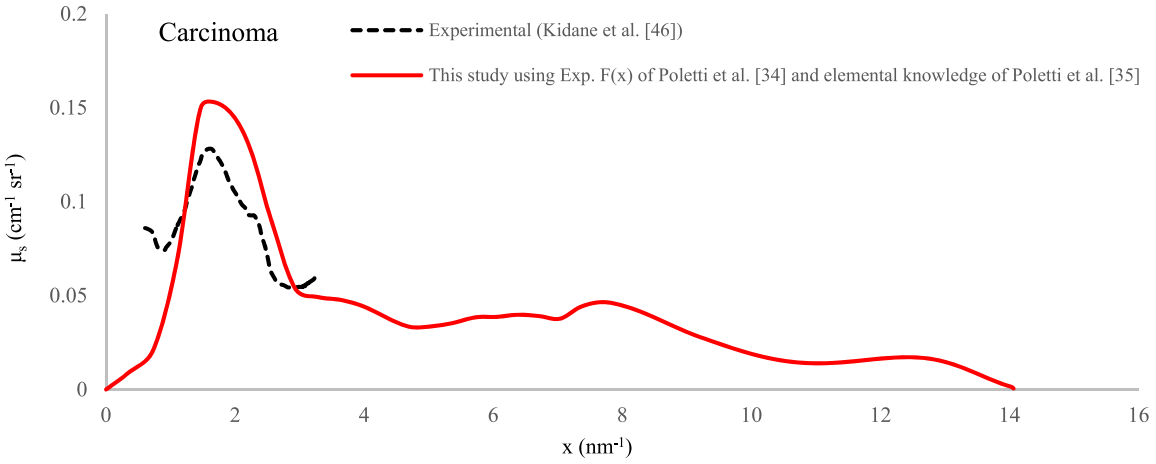

Fig. 3. Theoretical linear differential coherent scattering coefficients (μ_s) compared with experimental data in the literature for cancerous breast tissue.

in this study. The molecular coherent scattering cross-section was calculated with the use of data formed by combining both theoretical ($x > 8$ nm^{-1}) and experimental ($x \leq 8$ nm^{-1}) molecular form factors. It is very important to determine the photon attenuation coefficient as the sum of the coherent, incoherent, and photoelectric interactions, which are dominant in the interaction of the photon with the tissue, especially at energies between 1 and 50 keV. This study was compared with their experimental counterparts and was observed to be generally in good agreement.

Knowing the elemental content of the molecular structure that makes up the tissue makes it possible to calculate the attenuation coefficients. By knowing the attenuation coefficients correctly, the image that shows the difference between healthy tissue and tumor tissue is revealed, and with the increase in image quality, the amount of dose to be given to the patient will be adjusted more accurately. The results of this study can be used in the calculations of other modeling researchers and will shed light on experimental studies that have been or will be done. We strongly believe that our results will provide valuable information for breast tissue characterization and modeling in the MC code.

Declaration of competing interest

The author declares that there are no competing financial interests or personal relationships with other people or organizations that could have appeared to influence the work reported in this paper.

Acknowledgments

This research was supported by the Scientific and Technological Research Council of Turkey (TÜBİTAK) by grant no: 119F198.

References

[1] I. Akkurt, S. Al-Obaidi, H. Akyildirim, K. Gunoglu, Neutron shielding for ^{252}Cf source: FLUKA simulations, Iran J. Sci. Technol. Trans. Sci. 46 (2022) 1055.
[2] I. Akkurt, H.O. Tekin, Radiological parameters of bismuth oxide glasses using the PhyX/PSD software, Emerg. Mater. Res. 9 (2020) 1020.
[3] F. Kulali, Simulation studies on the radiological parameters of marble concrete, Emerg. Mater. Res. 9 (2020) 1341.
[4] R.B. Malidarre, I. Akkurt, Monte Carlo simulation study on TeO_2-Bi_20-PbO-MgO-B_2O_3 glass for neutron-gamma ^{252}Cf source, J. Mater. Sci. Mater. Electron. 32 (2021), 11666.
[5] M. Sarihan, Simulation of gamma-ray shielding properties for materials of medical interest, Open Chem. 20 (2022) 81.
[6] M. Ucar, H.F. Kayıran, A.V. Korkmaz, Gamma-ray-shielding parameters of carbon-aramid epoxy composites, Emerg. Mater. Res. 11 (2022) 338.
[7] F. Waheed, M. İmamoğlu, N. Karpuz, H. Ovalıoğlu, Simulation of neutrons shielding properties for some medical materials, Int. J. Comput. Exp. Sci. Eng. 8 (2022) 5.
[8] Z. Aygun, M. Aygün, An analysis on radiation protection abilities of different colored obsidians, Int. J. Comput. Exp. Sci. Eng. 9 (2023) 170.
[9] O. Günay, İ.N. Altıntaş, M. Demir, N. Yeyin, Dose calibrator measurements in the case of voltage fluctuations, Int. J. Comput. Exp. Sci. Eng. 9 (2023) 161.
[10] B. Oruncak, Computation of neutron coefficients for B2O3 reinforced composite, Int. J. Comput. Exp. Sci. Eng. 9 (2023) 50.
[11] R.B. Malidarre, H.O. Tekin, K. Gunoğlu, H. Akyıldırım, Assessment of gamma ray shielding properties for skin, Int. J. Comput. Exp. Sci. Eng. 9 (2023) 6.
[12] E.E. Altunsoy, H.O. Tekin, A. Mesbahi, I. Akkurt, MCNPX simulation for radiation dose absorption of anatomical regions and some organs, Acta Phys. Pol., A 137 (2020) 561.
[13] I. Akkurt, R.B. Malidarre, I. Kartal, K. Gunoğlu, Monte Carlo simulations study on gamma ray–neutron shielding characteristics for vinyl ester composites, Polym. Compos. 42 (2021) 4764.
[14] I. Akkurt, A.M. El-Khayatt, Effective atomic number and electron density of marble concrete, J. Radioanal. Nucl. Chem. 295 (2013) 633.
[15] I. Akkurt, Effective atomic and electron numbers of some steels at different energies, Ann. Nucl. Energy 36 (2009) 1702.
[16] I. Akkurt, Effective atomic numbers for Fe–Mn alloy using transmission experiment, Chin. Phys. Lett. 24 (2007) 2812.
[17] R. Kurtuluş, T. Kavas, I. Akkurt, K. Gunoğlu, H.O. Tekin, C. Kurtuluş, A comprehensive study on novel alumino-borosilicate glass reinforced with Bi2O3 for radiation shielding applications: synthesis, spectrometer, XCOM, and MCNP-X works, J. Mater. Sci. Mater. Electron. 32 (2021), 13882.
[18] G.R. Hammerstein, M.S. Daniel, W. Miller, D.R. White, M.E. Masterson, M.S. Helen, H.Q. Woodard, J.S. Laughlin, Absorbed radiation dose in mammography, Radiology 130 (1979) 485.
[19] H.Q. Woodard, D.R. White, The composition of body tissues, Br. J. Radiol. 59 (1986) 1209.
[20] D.R. White, L.H.J. Peaple, T.J. Crosby, Measured attenuation coefficients at low photon energies (9.88-59.32 keV) for 44 materials and tissues, Radiat. Res. 84 (1980) 239.
[21] P.C. Johns, M.J. Yaffe, X-ray characterization of normal and neoplastic breast tissues, Phys. Med. Biol. 32 (1987) 675.
[22] F.E. Carroll, J.W. Waters, W.W. Andrews, R.R. Price, D.R. Pickens, R. Willcott, P. Tompkins, C. Roos, D. Page, G. Reed, A. Ueda, R. Bain, P. Wang, M. Bassinger, Attenuation of monochromatic X-rays by normal and abnormal breast tissues, Invest. Radiol. 29 (1994) 266.
[23] J.S. Al-Bahri, N.M. Spyrou, Photon linear attenuation coefficients and water content of normal and pathological breast tissues, Appl. Radiat. Isot. 47 (1996) 777.
[24] R.C. Chen, R. Longo, L. Rigon, F. Zanconati, A. Pellegrin, F. De Arfelli, D. Dreossi, R.H. Menk, E. Vallazza, T.Q. Xiao, E. Castelli, Measurement of the linear attenuation coefficients of breast tissues by synchrotron radiation computed tomography, Phys. Med. Biol. 55 (2010) 4993.
[25] A. Tomal, I. Mazarro, E.M. Kakuno, M.E. Poletti, Experimental determination of linear attenuation coefficient of normal, benign and malignant breast tissues, Radiat. Meas. 45 (2010) 1055.
[26] A. Tomal, Medidas Experimentais dos Coeficientes de Atenuação de Tecidos Mamários e sua Influência no Contraste e Dose Mamográfica, Universidade de São Paulo Brazil, 2007.
[27] S. Mirji, N.M. Badiger, S.S. Kulkarni, P.B. Gai, M.K. Tiwari, Measurement of linear attenuation coefficients of normal and malignant breast tissues using synchrotron radiation, X Ray Spectrom. 45 (2016) 185.

[28] E. Fredenberg, F. Kilburn-Toppin, P. Willsher, E. Moa, M. Danielsson, D.R. Dance, K.C. Young, M.G. Wallis, Measurement of breast-tissue x-ray attenuation by spectral mammography: solid lesions, Phys. Med. Biol. 61 (2016) 2595.
[29] E. Fredenberg, P. Willsher, E. Moa, D.R. Dance, K.C. Young, M.G. Wallis, Measurement of breast-tissue x-ray attenuation by spectral imaging: fresh and fixed normal and malignant tissue, Phys. Med. Biol. 63 (2018), 235003.
[30] L.D.H. Soares, M.S.S. Gobo, M.E. Poletti, Measurement of the linear attenuation coefficient of breast tissues using polienergetic x-ray for energies from 12 to 50 keV and a silicon dispersive detector, Radiat. Phys. Chem. 167 (2020) 1, 167, 108226.
[31] ICRU (International Commission on Radiation Units and Measurements, Tissue Substitutes in Radiation Dosimetry and Measurement, ICRU Report vol. 44, Bethesda, MD: ICRU, 1989..
[32] G. Paterno, P. Cardarelli, M. Gambaccini, A. Taibi, Comprehensive data set to include interference effects in Monte Carlo models of x-ray coherent scattering inside biological tissues, Phys. Med. Biol. 65 (2020), 245002.
[33] ICRU (International Commission on Radiation Units and Measurements), Photon, Electron, Proton, and Neutron Interaction Data for Body Tissues, ICRP Report vol. 46, Bethesda, MD: ICRU, 1992..
[34] M.E. Poletti, O.D. Gonçalves, I. Mazzaro, X-ray scattering from human breast tissues and breast-equivalent materials, Phys. Med. Biol. 47 (2002) 47.
[35] M.E. Poletti, O.D. Gonçalves, I. Mazzaro, Coherent and incoherent scattering of 17.44 and 6.93 keV x-ray photons scattered from biological and biological-equivalent samples: characterization of tissues, X Ray Spectrom. 31 (2002) 57.
[36] J.H. Hubbell, Photon cross sections, attenuation coefficients, and energy absorption coefficients from 10 keV to 100 GeV, NSRDS-NBS 29 (1969).
[37] A. Böke, Linear attenuation coefficients of tissues from 1 keV to 150 keV, Radiat. Phys. Chem. 102 (2014) 49–59.
[38] J.H. Hubbell, I. Øverbø, Relativistic atomic form factors and photon coherent scattering cross sections, J. Phys. Chem. Ref. Data 8 (1979) 69.
[39] D. Schaupp, M. Schumacher, F. Smend, P. Rullhusen, J.H. Hubbell, Small angle Rayleigh scattering of photons at high energies: tabulations of relativistic HFS modified atomic form factors, J. Phys. Chem. Ref. Data 12 (1983) 467.
[40] J.H. Hubbell, W.J. Veigele, E.A. Briggs, R.T. Brown, D.T. Cromer, R.J. Howerton, Atomic form factors, incoherent scattering functions, and photon scattering cross sections, J. Phys. Chem. Ref. Data 4 (1975) 471.
[41] S.M. Midgley, Measurements of the X-ray linear attenuation coefficient for low atomic number materials at energies 32-66 and 140 keV, Radiat. Phys. Chem. 72 (2005) 525.
[42] D.R. White, E.M. Widdowson, H.Q. Woodard, W.T. Dickerson, The composition of body tissues, Br. J. Radiol. 64 (1991) 149.
[43] ICRP (International Commission on Radiological Protection), Report of the Task Group on Reference Man, in: ICRP Report, vol. 23, Pergamon, Oxford, 1975.
[44] D.E. Peplow, K. Verghese, Measured molecular coherent scattering form factors of animal tissues, plastics and human breast tissue, Phys. Med. Biol. 43 (1998) 2431.
[45] J. Kosanetzky, B. Knoerr, G. Harding, U. Neitzel, X-ray diffraction measurements of some plastic materials and body tissues, Med. Phys. 14 (1987) 526.
[46] G. Kidane, R.D. Speller, G.J. Royle, A.M. Hanby, X-ray scatter signatures for normal and neoplastic breast tissues, Phys. Med. Biol. 44 (1999) 1791.
[47] M.J. Berger, J.H. Hubbell, S.M. Seltzer, J. Chang, J.S. Coursey, R. Sukumar, D. S. Zucker, K. Olsen, XCOM: Photon Cross Sections Database, 2010.